



Fractal structure in the silver oxide thin film

S.M. Hou^a, M. Ouyang^a, H.F. Chen^a, W.M. Liu^a, Z.Q. Xue^{a,*}, Q.D. Wu^a, H.X. Zhang^b,
H.J. Gao^b, S.J. Pang^b

^a Department of Electronics, Peking University, Beijing 100871, China

^b Beijing Laboratory of Vacuum Physics, Beijing 100080, China

Received 10 April 1997; accepted 4 August 1997

Abstract

The first two steps of the preparation of Ag–O–Cs photocathodes are the deposition of silver films and their oxidation with the glow discharge method. The fractal structure and texture structure in the silver oxide thin film have been characterized by transmission electron microscopy (TEM). The Hausdorff dimension D of the fractal structure is calculated to be 1.80 ± 0.01 . The formation mechanism of the fractal structure is also discussed. © 1998 Elsevier Science S.A.

Keywords: Fractal; Transmission electron microscopy (TEM); Texture structure; Silver oxide

1. Introduction

Fractal, which was first introduced by Benoit Mandelbrot in 1973, has been extensively used in mathematics, physics, chemistry, geography, etc. A lot of books and papers about the theory and application of fractal have been published [1–3]. Many results demonstrate that fractal structure is a state between order and disorder, which is unstable or metastable. Fractal structures exist in the world widely.

The Ag–O–Cs photocathode, which is called S-1 photocathode by the Joint Electron Device Engineer Committee (JEDEC) of the United States, is the first practical photocathode invented in 1929 and is still used now. S-1 photocathode is very sensible in visible and near infrared range [4], and has a rapid response speed in the near infrared ultrashort laser pulse detection [5]. The oxidation step of silver thin films is an important stage in the preparation of S-1 photocathode. There are many reports of fractal structures in thin films [6–8]. In this paper, we present a fractal structure of the silver oxide thin film fabricated in vacuum.

2. Experiments

In the preparation of silver oxide thin films, the first step is the deposition of silver thin films by a vacuum thermal evaporation method. The base vacuum of the deposition system is about 5×10^{-5} Pa. For analyzing thin films with transmission electron microscopy (TEM), amorphous SiO₂ thin films are adopted as supporting films of the TEM samples. Copper grids are placed on a movable magnetic support in a glass tube. Silver thin films are simultaneously deposited onto the inside of the glass tube and SiO₂ supporting films, so their thickness can be controlled by the transmissivity of white light. In order to study silver oxide thin films at different growth stages, copper grids can be moved out of the deposition region at different values of transmissivity, thus silver thin films with different thickness can be prepared. The deposition process of silver thin film is usually stopped when the light transmissivity drops at 30 ~ 70%.

The second step is the oxidation of silver thin films. The pressure in the tube is raised at about 10 Pa by introducing pure oxygen gas. The oxygen gas in the tube is ionized with the glow discharge method. The voltage of the AC power supply is 600 V, and the frequency is 50 Hz. Silver thin films are bombarded by positive and nega-

* Corresponding author.

tive oxygen ions and oxidized. The main component in silver oxide thin films is Ag_2O , but Ag_2O_2 also exists. Because Ag_2O is transparent for visible light, the oxide process can be controlled by the transmissivity increase of silver thin films. When the transmissivity is raised to about 100% [4], the glow discharge is interrupted. Silver thin films are at room temperature during the oxidation process. There are other steps in the preparation of Ag–O–Cs photocathode, but we stop here in order to study the structure of silver oxide thin film. Samples of silver oxide thin films are examined by a JEOL JEM-200CX TEM operated at 160 kV.

3. Results and discussions

Figs. 1 and 2 are both TEM micrographs of silver oxide thin films at different stages. The light transmissivity drops at 65% and 30% before silver thin films are oxidized. When the light transmissivity is raised to about 80%, they are moved out of the glow discharge region. Both of their diffraction rings are a superposition of silver diffraction rings and silver oxide diffraction rings. From inner to outer, the diffraction rings in Fig. 1 are indexed as $\text{Ag}_2\text{O}\{111\}$, $\text{Ag}\{111\}$, $\text{Ag}\{200\}$, $\text{Ag}_2\text{O}\{220\}$, $\text{Ag}\{220\}$ and $\text{Ag}\{311\}$. There are more silver diffraction rings in Fig. 2. The diffraction rings are $\text{Ag}_2\text{O}\{111\}$, $\text{Ag}\{111\}$, $\text{Ag}\{200\}$, $\text{Ag}_2\text{O}\{220\}$, $\text{Ag}\{220\}$, $\text{Ag}\{311\}$, $\text{Ag}\{222\}$, $\text{Ag}\{400\}$, $\text{Ag}\{331\}$ and $\text{Ag}\{420\}$. Both of them are not oxidized enough. The size of clusters in Fig. 1 is about 20 nm in diameter. Little silver grains have only been oxidized on their surface known form the diffraction pattern. There is no discrete diffraction spots in the diffraction pattern of Fig. 1, which indicates that silver grains have no preferred orientation. The silver oxide thin film in Fig. 2 has been a continuous film. Those discrete diffraction spots in its diffraction pattern indicate that there are preferred orientation when the silver film is formed.

Fig. 3 shows a fractal structure of silver oxide thin film and its selected area electron diffraction pattern. The light transmissivity drops at 30% before the silver thin film is oxidized; when the transmissivity is raised to about 100%, the glow discharge is interrupted. Seen from the micrograph, it is an open structure with dendritic arms, showing a typical fractal character. Its selected area diffraction pattern is a texture structure with a sixfold symmetry.

Texture structures are discussed in some books [9,10]. It belongs to a polycrystal aggregate with preferred orientations. There is a special crystal axis aligning along some direction (the texture axis), other orientations round this axis are aligning randomly. Usually, there is an identical crystal plane parallel to the substrate surface in each grain of the polycrystal thin film. The method to rotate the reciprocal lattice can be adopted to discuss the diffraction pattern. If the electron beam incidents along the direction of the texture axis $[uvw]$, the diffraction rings $\{hkl\}$ which satisfy $hu + kv + lw = 0$, can appear concerning the diffraction pattern center. For example, in the face-centered structure, if $[uvw] = [111]$, then $h + k + l = 0$, diffraction rings such as $\{111\}$, $\{200\}$, $\{311\}$, $\{222\}$, $\{331\}$, $\{420\}$ vanish, only diffraction rings such as $\{2\bar{2}0\}$, $\{4\bar{2}2\}$, $\{4\bar{4}0\}$ can be observed. If there is an angle between the electron beam and the texture axis, the diffraction ring will be broken into a series of arcs and their centers will be arranged in a few lines.

In the center of the diffraction pattern shown in Fig. 3, there is a circular white spot with a hexagonal grey spot in it. Outside the white spot, there are two circular rings composed of six arcs. The six arcs of the ring with a smaller radius, which are located along the directions of the six vertex angles of the grey spot, are more observable. The six arcs of the larger ring are weaker, and they appear between the directions of the six vertex angles of the grey spot. From these characteristics of the diffraction pattern, it can be guessed that the electron beam incidents along the direction of the texture axis, and that there are statistically

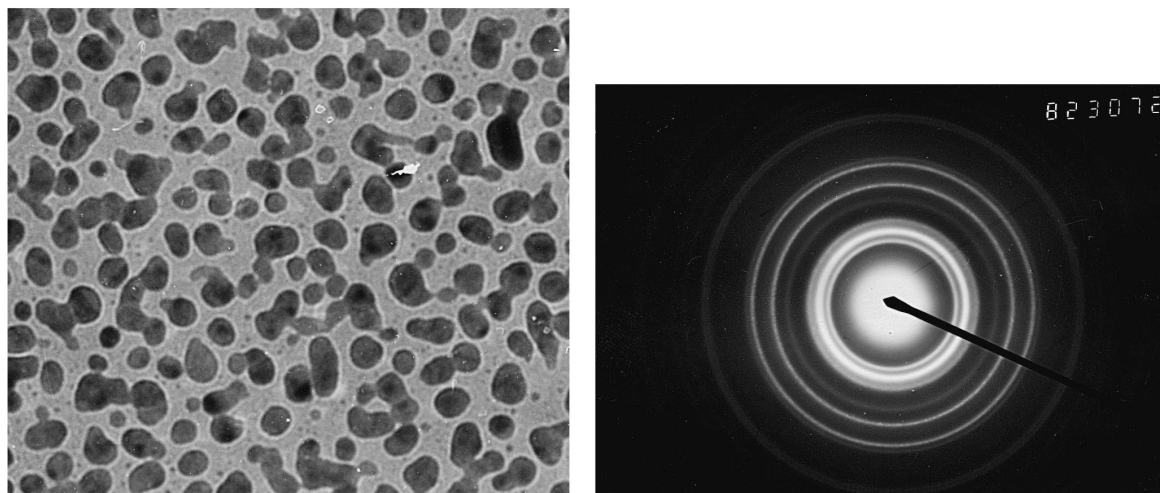


Fig. 1. TEM micrograph of silver oxide thin film in an early stage. (a) TEM micrograph, magnification: 3×10^4 . (b) Its selected area diffraction pattern.

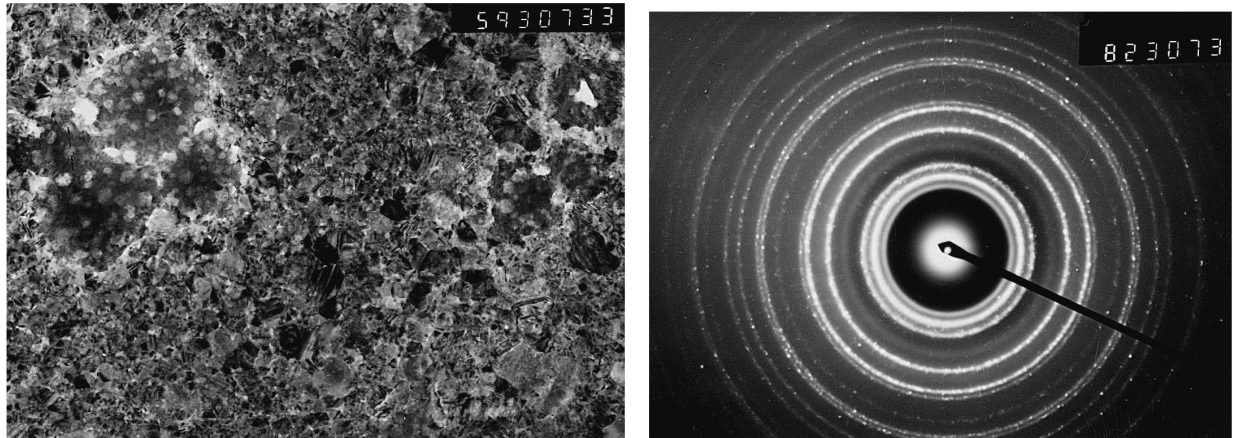


Fig. 2. TEM micrograph of silver oxide thin film at a continuous film stage. (a) TEM micrograph, magnification: 3×10^4 . (b) Its selected area diffraction pattern.

preferred orientations perpendicular to the texture axis in the silver oxide thin film so that the arcs have a sixfold symmetry. The ratio of the square of the radii of the three diffraction rings is 4:11:16, so the diffraction rings are

indexed $\text{Ag}_2\text{O}\{002\}$, $\text{Ag}_2\text{O}\{1\bar{1}3\}$ and $\text{Ag}_2\text{O}\{004\}$, respectively, and the texture axis is $[110]$. The bright part of the micrograph is Ag_2O film, which is determined to be a fractal structure.

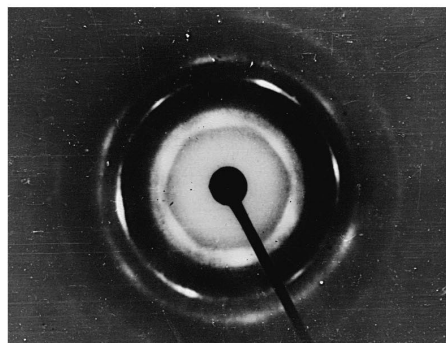


Fig. 3. Texture structure of silver oxide film. (a) TEM micrograph, magnification: 5×10^4 . (b) Its selected area diffraction pattern.

In order to compute the fractal dimension of the silver oxide thin film, we use the following image process of the TEM micrograph. Firstly, we digitize the micrograph of Fig. 3 using a HP Jet Scanner at 250 DPI resolution, the image is 1109 pixels long and 751 pixels wide, each pixel has a grey value ranged from 0 to 255. Secondly, an appropriate threshold is selected to separate the feature and the background. Since pixels have a finite size, they average the values from both sides of the boundaries they straddle. But the act of segmenting the image requires assigning each pixel to either the feature or the background. Thus the selection of threshold becomes an important question. Fig. 4 is the computer processing results of Fig. 3. Known from the histogram of pixel grey value distribution, the correct threshold must lie in the two peaks, which correspond to the feature and the background. There is a broad valley between the two peaks, the threshold selected at different positions must give different results. In this paper, 154, 127 and 100 are selected as the thresholds to process the image, and the two-value pictures are printed. The picture of threshold at 127 is the most similar to the original image and the difference among them is very little, Fig. 4b is the two-value picture of threshold at 127.

The fractal dimension is determined by the measure relation. We consider a series of concentric circles whose center is the pixel grey value distribution center of the

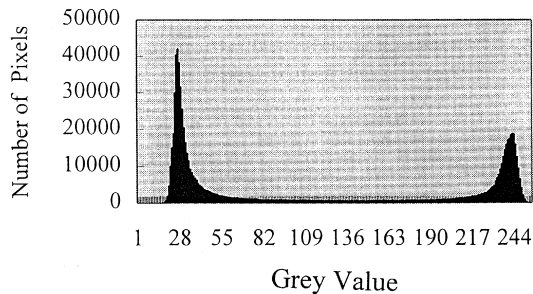


Fig. 4. Computer treated results of Fig. 3a. (a) The histogram of pixel grey value distribution. (b) The two-value graph of threshold as 127.

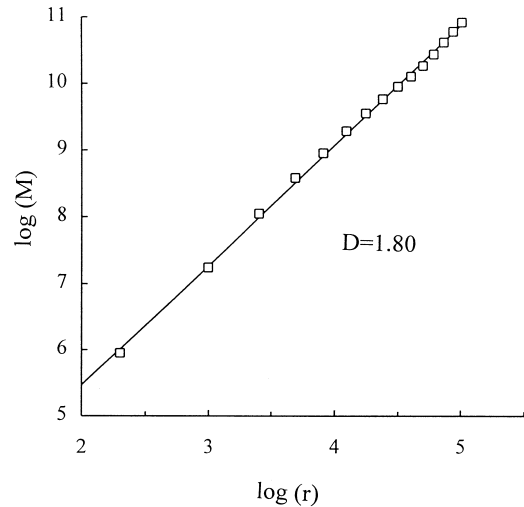


Fig. 5. The Log vs. Log plot of M and r of the threshold as 127.

feature, the total number of pixels M belonging to the feature in a circle is counted. If the pixel distribution function M satisfies the relation $M(r) \propto r^D$ for different radii r , the feature is a D -dimensional fractal structure. According to our image, a series of rectangles with the same center are selected, whose center is also the pixel grey value distribution center of the feature, whose widths are $4 \times r$ and whose lengths are $(1109/751) \times 4r$, the step of r is 10. Fig. 5 shows the pixel distribution function $M(r)$ dependence of r in the double log scale coordination system at the threshold of 127. The data of M vs. r satisfy a power function very well. The linear fitting of the data gives the dimension as 1.80. The figures of $M(r)$ dependence of r in the double log scale coordination system at the threshold of 154 and 100 have been obtained, using the same method. The slope of the linear fitting line is 1.81 and 1.79. Though the dimension is different at different thresholds, the difference is not very big. The fractal dimension is determined to be 1.80 ± 0.01 .¹

Much efforts have been devoted to study the growth mechanism of fractal structures. The diffusion-limited aggregation (DLA) model [11,12] and the diffusion-limited cluster aggregation (DLCA) model [13,14] are usually adopted to explain fractal structures. The dimension of the fractal structure generated using DLCA model in three dimensions is about 1.80. The fractal dimension is also about 1.80 when the fractal structure is projected into two dimensions, using the fact that the fractal dimension remains unchanged upon projection provided $D \leq 2$ [15]. Because the examination of the feature is based on the TEM micrograph, our analysis is performed for a two-dimensional diffraction contrast image of the thin film sam-

¹ The standard deviation of fractal dimension was obtained using the formula on p. 50 of Ref. [3].

ple. Our result is in remarkable agreement with the computer simulations. But there is an obvious difference in the growth process between our result with the computer simulations. The clusters and particles move equally in all directions in computer simulations. But the deposited silver thin films are polycrystal films. Oxygen ions easily diffuse along the interfaces among silver grains. In the oxidation process, little silver grains are oxidized first on their surface. When oxidized continually, little silver grains become smaller and silver oxide films become thicker. So progressive study is needed to know how to form the fractal and texture structure during the oxidation process of silver thin films.

4. Conclusion

Silver oxide thin films are prepared and their structure properties are studied by TEM. The deposited silver thin films are polycrystal films. Fractal and texture structure are observed, and the fractal dimension is 1.80 ± 0.01 . The oxidation of silver thin film is an important step in the preparation of Ag–O–Cs photocathode. The physical and photoemissive properties of Ag–O–Cs photocathodes depend on their microstructures, so the study of the microstructure of silver oxide thin film is helpful to explain the optical and electrical characters of Ag–O–Cs photocathodes.

Acknowledgements

The authors are indebted to Mr. Liu Limin and Mr. Hu Xinyu for a beneficial discussion of image process. This work was partially supported by Natural Science Foundation of China (No. 69701001).

References

- [1] J. Feder, *Fractals*, Plenum, New York, 1988.
- [2] V. Tamas, *Fractal Growth Phenomena*, World Scientific, Singapore, 1992.
- [3] J.C. Russ, *Fractal Surfaces*, Plenum, New York, 1994.
- [4] A.H. Sommer, *Photoemissive Materials—Preparation, Properties, and Uses*, Wiley, New York, 1968.
- [5] M.Ya. Schelev, *SPIE* 348 (1982) 75.
- [6] P. Bieganski, E. Dobierzewska-Mozrzyms, M. Newelski, E. Pieciul, *Vacuum* 46 (1995) 513.
- [7] H.J. Gao, Z.Q. Xue, Q.D. Wu, S. Pang, *J. Mater. Res.* 9 (1994) 2216.
- [8] A. Kapitulnik, G. Deutscher, *Phys. Rev. Lett.* 49 (1982) 1444.
- [9] H.E. Marr, *Electron Optical Applications in Materials Science*, McGraw-Hill, New York, 1970.
- [10] P. Hirsch, A. Howie, R.B. Nicholson, D.W. Pashley, M.J. Whelan, *Electron Microscopy of Thin Crystals*, Robert E. Krieger Huntington, New York, 1977.
- [11] T.A. Witten, L.M. Sander, *Phys. Rev. Lett.* 47 (1981) 1400.
- [12] T.A. Witten, L.M. Sander, *Phys. Rev. B* 27 (1983) 5686.
- [13] P. Meakin, *Phys. Rev. Lett.* 51 (1983) 1119.
- [14] P. Meakin, *Phys. Rev. A* 27 (1983) 604.
- [15] B.B. Mandelbrot, *The Fractal Geometry of Nature*, Freeman, San Francisco, CA, 1982.